

## Supporting Information

### Efficient removal of copper ion through photothermal enhanced flow-electrode capacitive deionization

Mengyao He<sup>#</sup>, Jiaqi Chen<sup>#</sup>, Ziquan Wang<sup>#</sup>, Zengye Chen, Libo Deng\*

#### Experimental Section

##### Chemicals and materials

The zinc acetate dihydrate ( $C_4H_6O_4Zn \cdot 2H_2O$ , 98%), 2-methylimidazole ( $C_4H_6N_2$ , 98%), potassium hydroxide (KOH, 95%), polyvinylidene fluoride (PVDF), and polyvinylpyrrolidone (PVP, AMW: 58000) were purchased from Macklin biochemical Co., Ltd. The sodium chloride (NaCl, 99.5%), cupric chloride anhydrous ( $CuCl_2$ , 98%) and N-methyl-2-pyrrolidone (NMP, 99%) were purchased from Shanghai Aladdin Biochemical Technology Co., Ltd. Hydrochloric acid (HCl) was purchased from China National Pharmaceutical Group Co., Ltd. Conductive carbon black (Vulcan XC-72R) was purchased from Cabot Corporation. Corresponding standard solutions were purchased from Guobiao (Beijing) Testing & Certification Co., Ltd. All chemicals were used as received without further purification. Deionized water was lab-made by an ultrapure water system (YOUPU UPHC-I-90T, Chengdu China) with a conductivity below  $18 M\Omega cm$ .

##### Preparation of materials

###### *Synthesis of ZIF*

First, 18 g of 2-methylimidazole was added to 500 mL of deionized water to form solution A. Then 12 g zinc acetate was dissolved in 500 mL deionized water to form solution B. Solutions A and B were fully mixed and continuously stirred for 12 hours to form a dark gray precipitate. Finally, after three centrifuges at 5000 rpm, the

precursor of ZIF-C-K was obtained, denoted as ZIF.

### *Synthesis of ZIF-C-K*

A proper amount of ZIF was added to a quartz crucible and heated to 800 °C at a heating rate of 5 °C min<sup>-1</sup> in a tube furnace under a nitrogen atmosphere, maintained for 2 hours, and naturally cooled to room temperature to obtain ZIF-C. Next, a certain amount of ZIF-C was dispersed in 40 mL of deionized water, and the same mass of KOH was added and stirred for 12 hours. The thoroughly stirred mixture was dehydrated by using an oil bath at 100 °C. Finally, the obtained powder was transferred to a nickel crucible, heated to 800 °C at a heating rate of 5 °C min<sup>-1</sup> in a tube furnace under a nitrogen atmosphere, maintained for 2 hours, and naturally cooled to room temperature. The resulting product was immersed in 1 M HCl and stirred vigorously for 12 hours. It was then washed with plenty of deionized water until pH=7, dried at 70 °C in a forced air oven for 12 hours, and named ZIF-C-K.

### **Structural characterization**

The morphology and microstructure of the samples were characterized by field emission scanning electron microscopy (FE-SEM, JSM-7800F&TEAM Octane Plus, Japan) and transmission electron microscopy (TEM, JEM-2100&X-Max80, Japan). The specific surface area (SSA) of the samples was evaluated using N<sub>2</sub> adsorption-desorption isotherms at 77 K and liquid nitrogen as adsorbent (ASAP-3Flex, Micromeritics, USA) by the Brunauer-Emmett-Teller (BET) method and the pore size was analyzed using a density function model (DFT). Raman spectroscopy was collected using a Raman spectrometer (Raman, Renishaw INVIA REFLEX, UK) equipped with a 532 nm laser, a 50X objective, and the laser energy is 5%. The chemical compositions of the samples were evaluated using X-ray photoelectron spectroscopy (XPS, K-Alpha<sup>+</sup>, UK) with a monochromatic Al K $\alpha$  X-ray source. All high-resolution spectrums were calibrated by the C1s peak located at 284.8 eV. The structural analysis of the samples was conducted using X-ray powder diffraction (XRD, PANalytical Empyrean, Netherlands), equipped with Cu K $\alpha$  radiation. The ion concentrations were measured using inductively coupled plasma

atomic emission spectrometry (ICP-AES, ICP-Avio 200, PE Instruments, USA). The  $R^2$  values for all calibration curves are above 0.999.

### Electrochemical measurements

We used an electrochemical workstation (CHI760E, Shanghai Chenhua Instrument Co., Ltd., China) for electrochemical characterization. The potential window for cyclic voltammetry (CV) measurements is  $-1-0$  V (relative to Ag/AgCl). The scanning rate varies between  $100 \text{ mV s}^{-1}$  and  $1 \text{ mV s}^{-1}$ , using 1M NaCl as the supporting electrolyte. The voltage window of the galvanostatic charge/discharge tests (GCD) is  $-1-0$  V and the current density is  $0.5-20 \text{ A g}^{-1}$ . Eq. 1 was used to calculate the specific capacitance ( $C_s$ ) of the material:

$$C_s = \frac{I\Delta t}{m\Delta V} \quad (1)$$

where  $m$  is the mass of active material (g),  $I$  is the applied current (A),  $\Delta t$  is the discharge time (s), and  $\Delta V$  is the potential range (V). The EIS tests were conducted in the frequency range from  $10^5$  to  $10^{-2}$  Hz at steady-state open circuit potential (OCP) by applying a small sinusoidal signal with an amplitude of 5 mV.

### FCDI system performance evaluation

The FCDI tests were conducted in the constant voltage mode, while current was recorded in real-time. The average salt removal rate (ASRR,  $\mu\text{g cm}^{-2} \text{ min}^{-1}$ ), energy consumption (EC,  $\text{J mg}^{-1}$ ) and charge efficiency (CE, %) were utilized to evaluate the FCDI performance. ASRR, EC and CE can be expressed as Eq. 2 to Eq. 4:

$$ASRR = \frac{[(C_{d,0} - C_{d,t}) + (C_{c,t} - C_{c,0})] \cdot V_s}{A \cdot t} \quad (2)$$

$$EC = \frac{\int IUdt}{[(C_{d,0} - C_{d,t}) + (C_{c,t} - C_{c,0})] \cdot V_s} \quad (3)$$

$$CE = \frac{n_x \cdot F \cdot V_s \cdot [(C_{d,0} - C_{d,t}) + (C_{c,t} - C_{c,0})]}{1000 \cdot M \cdot \int Idt} \quad (4)$$

where  $C_{d,0}$  and  $C_{d,t}$  is the initial concentration ( $\mu\text{g L}^{-1}$ ) and the concentration ( $\mu\text{g L}^{-1}$ ) at time  $t$  (min) of desalination chamber.  $C_{c,0}$  and  $C_{c,t}$  is the initial concentration ( $\mu\text{g L}^{-1}$ ) and the concentration ( $\mu\text{g L}^{-1}$ ) at time  $t$  (min) of concentration chamber.  $V_s$  represents the volume of the salt solution (L),  $A$  is the effective contact area between the flowing electrode and ion exchange membrane ( $16\text{ cm}^2$ ),  $U$  is the applied voltage (V),  $I$  is the current (A),  $M$  is the molar mass of the  $\text{Cu}^{2+}$  ( $63.55\text{ g mol}^{-1}$ ),  $F$  is the Faraday constant ( $96485\text{ C mol}^{-1}$ ), and  $n_x$  is the ion charge.

### **Flow capacitive deionization (FCDI) system configuration**

The FCDI system constructed in this study consisted of four chambers (*i.e.*, two flow electrode chambers, a desalination chamber, and a concentration chamber), two organic glass plates, two graphite plates (worked as current collectors), and ion exchange membranes (CEM: Fumasep FKS-50, Germany; AEM: standard type AMX, Japan). It is worth noting that we used 8107 perfluorosulfonic acid cation exchange membranes (Hangzhou Lvhe Environmental Protection Technology Co., Ltd, China) in the subsequent heat field enhanced FCDI system because it could ensure stable operations at higher temperatures. Silicone rubber gaskets were placed between each pair of plates to prevent water leakage. The graphite collectors were engraved with 2 mm wide and 2 mm deep flow channels with an effective contact area of  $16\text{ cm}^2$ , which can effectively promote the contact between the electrode slurry and the current collector. The flowing electrode slurry with a solid content of 3 wt.% was prepared by mixing 1.5 g of active material with 48.5 mL of salt solution (the initial concentration of the ion is identical to that in the desalination chamber). The FCDI system was operated in a short-circuit closed-loop mode (SCC), and the water supply was in a batch mode. The flow rate of the salt solution in the desalination and concentration chambers was  $20\text{ mL min}^{-1}$ , and the flow rate of the flowing electrode was  $30\text{ mL min}^{-1}$ .

To determine the optimal operating configurations, various voltages (1-2.5 V), flowing electrode mass loading ratios (1-7 wt.%), and initial ion concentrations (100-400 ppm  $\text{Cu}^{2+}$ ) were systematically studied. In a typical FCDI test, the initial

solution configuration in the desalination and concentration chamber was 200 ppm  $\text{Cu}^{2+}$  in 200 mL deionized water. A constant voltage was applied to the FCDI cell using an electrochemical workstation for 5 hours. To measure the concentration changes of ions during the test, 0.5 mL of solution was taken from the desalination chamber and the concentration chamber respectively every hour, diluted, and analyzed using inductively coupled plasma atomic emission spectrometry (ICP-AES).

### **FCDI experiments in a low-temperature environment**

An ice bath was employed to maintain the environmental temperature at 5 °C. Firstly, we added the pre-frozen ice to about 500 mL of deionized water to attain the ice-water mixture. Then this mixture was transferred to a thermostatic magnetic stirrer with a setting temperature of 5 °C. Subsequently, the baker containing the electrode slurry was placed in the stirrer and the FCDI experiment was conducted after the temperature stabilized at 5 °C.

### **EIS measurements with DRT analysis**

The KK-validated EIS data were then converted to distribution of relaxation times (DRT) plots using DRT tools by MATLAB R2023a, following Eq. 5:

$$Z(\omega) = R_{\infty} + R_{\text{pol}} \int_0^{\infty} \frac{\gamma(\tau)}{1 + j\omega\tau} d\tau \quad (5)$$

where  $Z(\omega)$  is the KK-validated impedance data obtained from the EIS measurements,  $R_{\infty}$  is the ohmic resistance,  $R_{\text{pol}}$  is the overall polarization resistance of the real part of the impedance and  $j$  is the complex unit. The function  $\gamma(\tau)$  is the normalized distribution of the relaxation time. The resistance of the peaks was calculated by integrating the peak area of the function  $\gamma(\ln(\tau))$ . The resistance contribution was calculated by dividing the resistance value of the investigated peak to the total resistance.

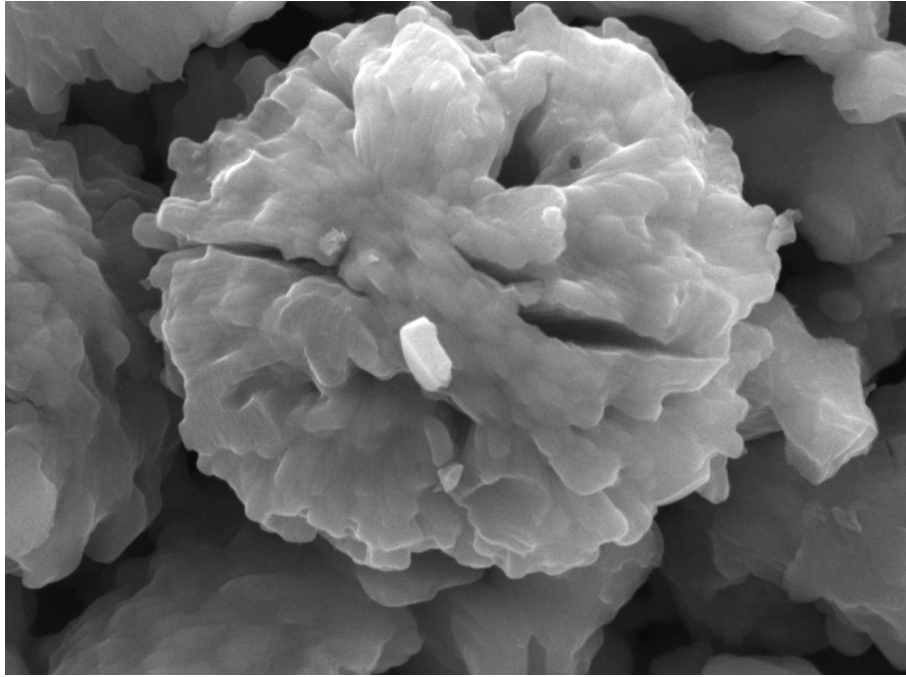


**Fig. S1** SEM image of ZIF-C

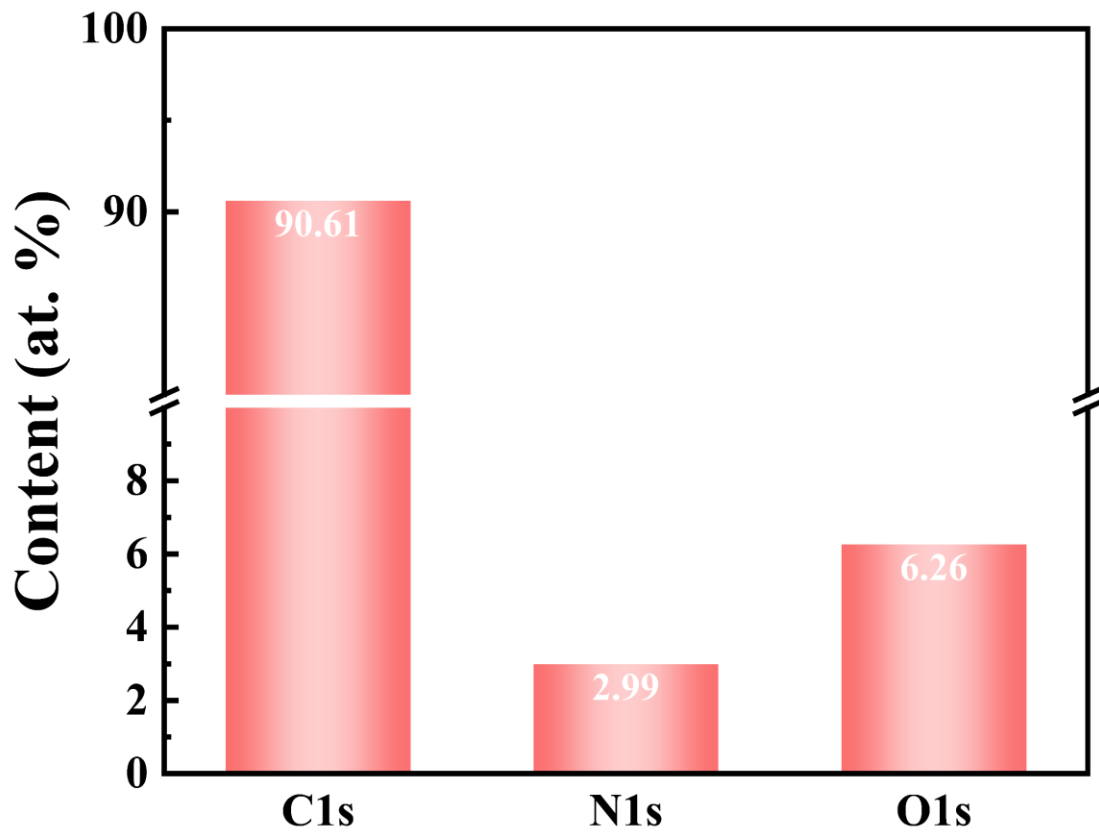


**Fig. S2** Element content of ZIF-C-K

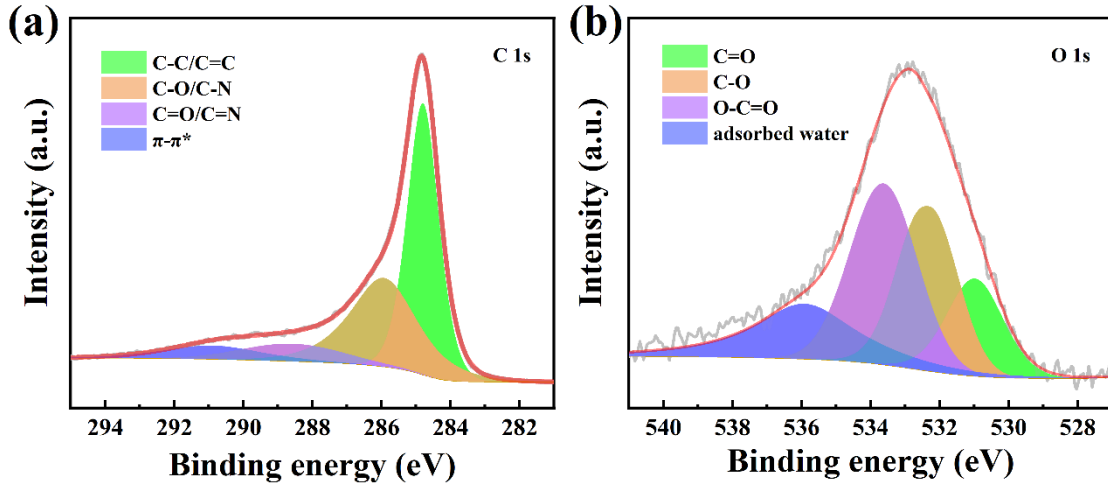


Fig. S3 High-resolution spectra of XPS: (a) C 1s and (b) O 1s

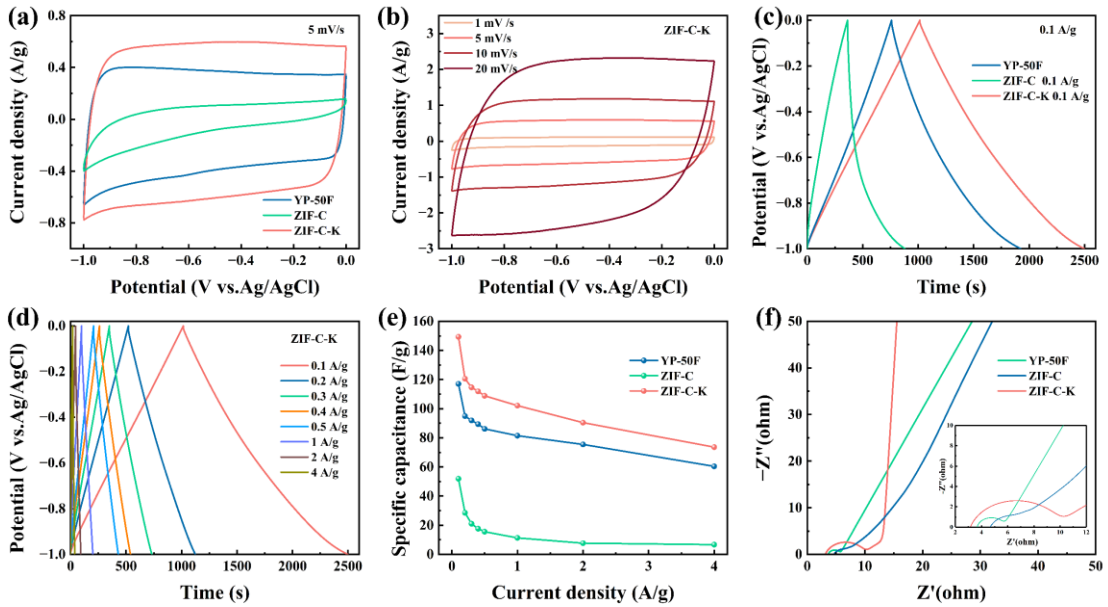


Fig. S4 CV curves of: (a) different materials at  $5 \text{ mV s}^{-1}$  and (b) ZIF-C-K at different scan rates; (c) GCD curves for different materials at  $0.1 \text{ A g}^{-1}$ ; (d) GCD curves for ZIF-C-K at different currents; (e) The relationship between specific capacitance and current density; (f) Nyquist plots.

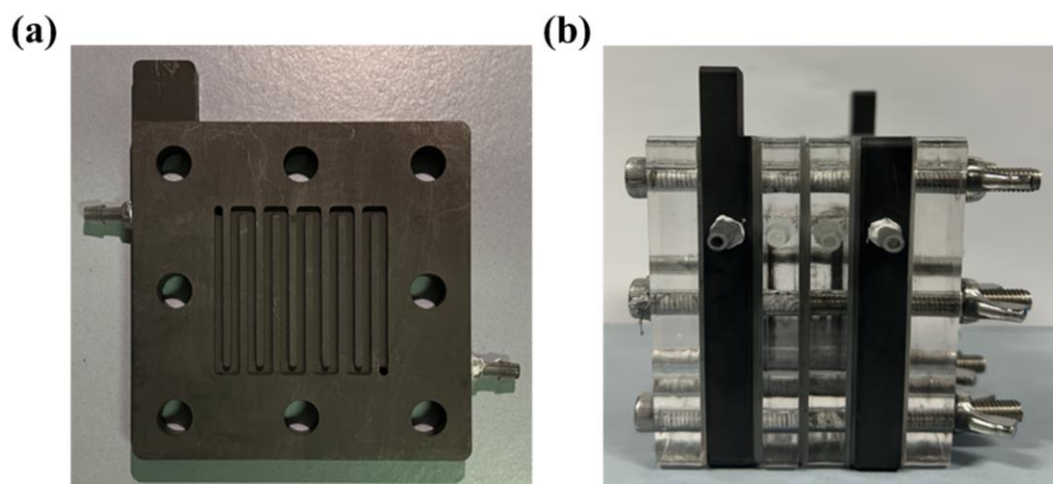


Fig. S5 Photographs of the FCDI setup

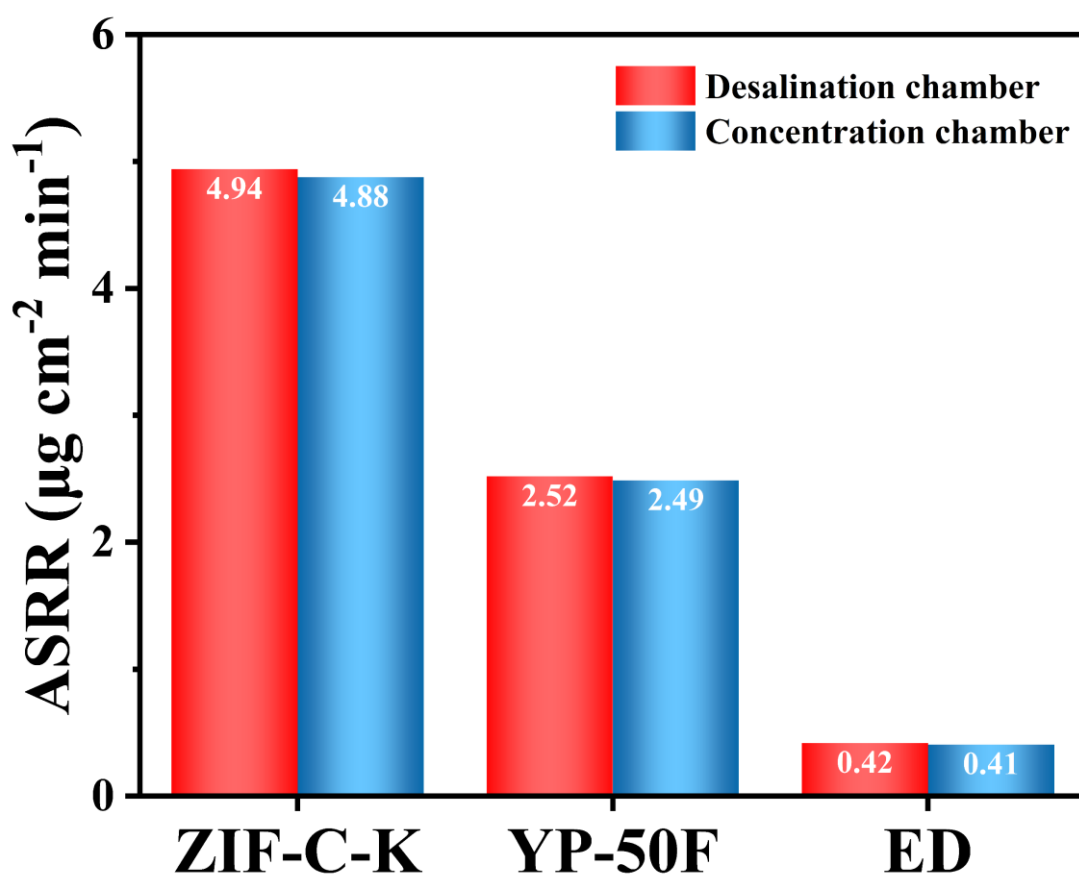


Fig. S6 ASRR achieved using electrodes consisting of different materials and electro dialysis (ED).



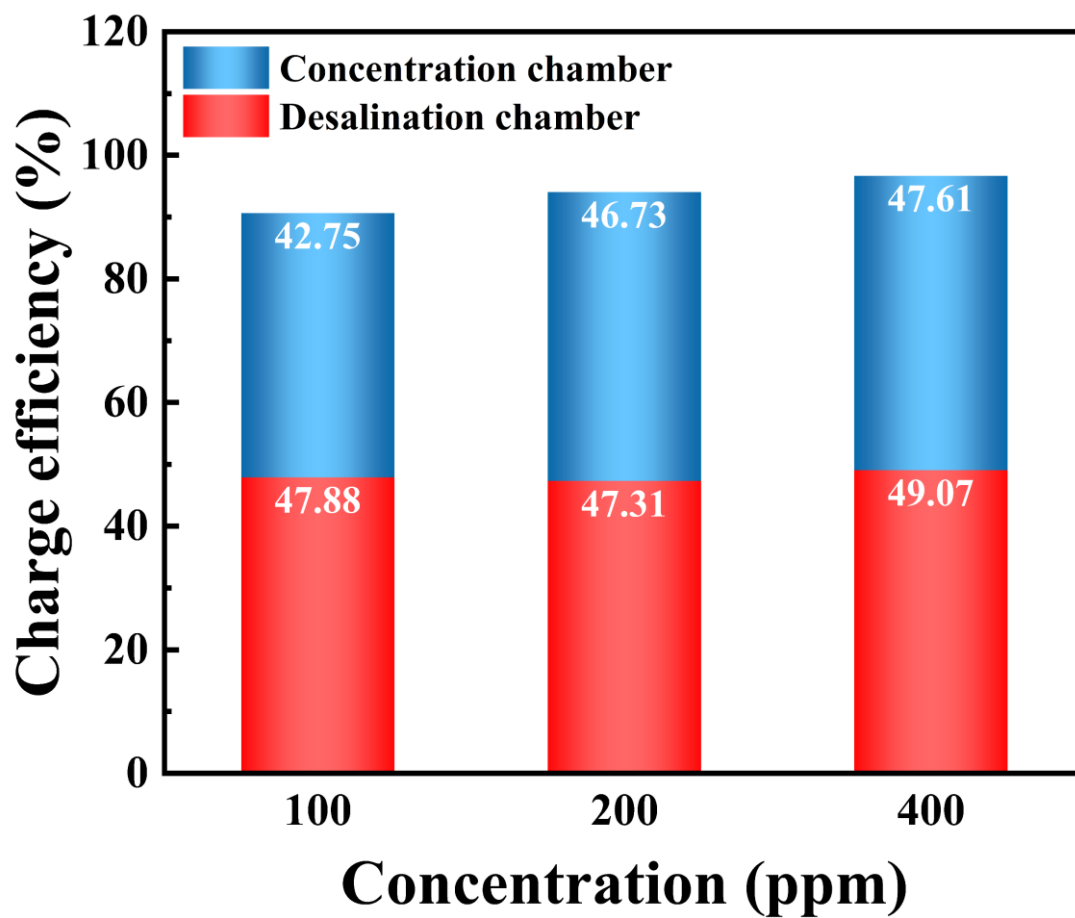


Fig. S7 Charge efficiency of the desalination and concentration chambers.

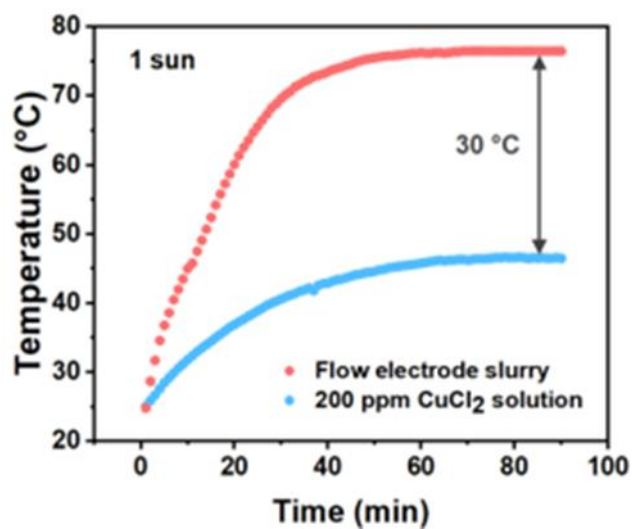


Fig. S8 Temperature evolution of the flowing electrode and the salt solution under 1 sun solar density.

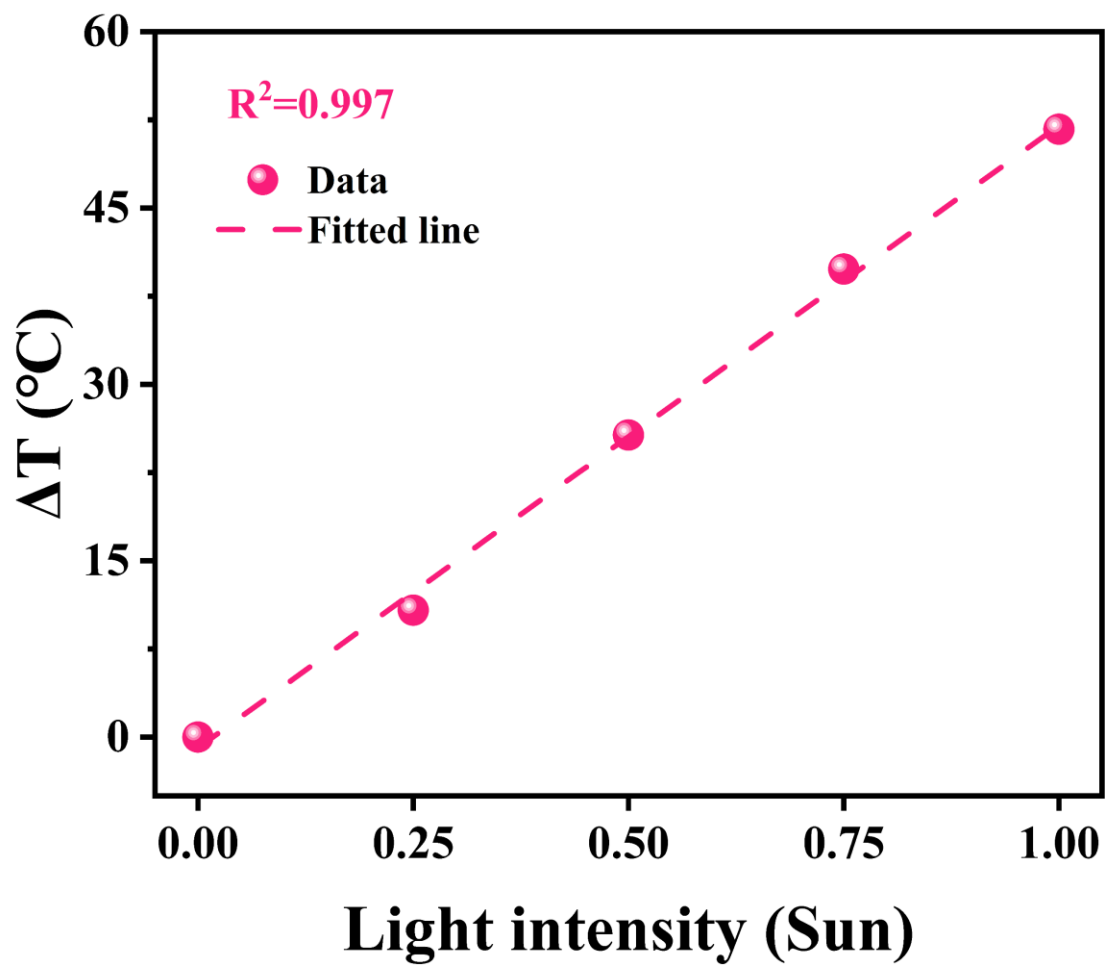


Fig. S9 The linear relationship between the saturated temperature and the light intensity.



Fig. S10 Photograph of the low temperature FCDI device.

